# Technique Development and Measurement of Poisson's Ratio, Lateral Creep Behavior, and Thermal and Hygroscopic Expansion of Individual Layers in Magnetic Tapes

**Tiejun Ma, Bharat Bhushan**

*Nanotribology Laboratory for Information Storage and MEMS/NEMS, The Ohio State University, 206 W. 18th Avenue, Columbus, Ohio 43210*

Received 20 April 2002; accepted 15 July 2002

**ABSTRACT:** An experimental technique was developed to measure the Poisson's ratio (lateral contraction over longitudinal elongation), lateral creep, and both thermal and hygroscopic expansion of thin polymeric films. A so-called profile-matching method was developed to measure the lateral and longitudinal deformation with the help of a laser scan micrometer. A thermomechanical analyzer was used to measure the coefficient of thermal expansion (CTE). The laser scan technique was also used to measure the coefficient of hygroscopic expansion (CHE). The measurements were performed on magnetic tapes, substrates, and tapes with front coat or back coat, or with both coats stripped. A model based on the rule of mixtures was developed to determine the Poisson's ratio, lateral and longitudinal deformation behavior, and thermal expansion of the front coat and back coat. To investigate the mechanical degradation of the substrates during tape manufacturing, the data for substrate with the front and back coats removed from the tape, were compared with the data for the never-coated virgin film. The relationship between the molecular structure and the degradation mechanism of the substrates is discussed. The magnetic tapes used in this research include two metal particle (MP) tapes and two metal evaporated (ME) tapes that use polyethylene terephthalate (PET) and polyethylene naphthalate (PEN) substrates. Longitudinal and lateral deformation tests were performed at 25 ± 0.5°C and 50 ± 2%RH, and thermal expansion was measured from 15 to 70°C. The CHE was measured at 25 ± 0.5°C and 15–80%RH. © 2003 Wiley Periodicals, Inc. J Appl Polym Sci 88: 2082–2096, 2003

**Key words:** magnetic tape; polymer film; Poisson's ratio; coefficient of thermal expansion; rule of mixtures

## INTRODUCTION

Magnetic tapes provide extremely high volumetric density, high data rates, and low cost per megabyte compared to that of other storage media. These are primarily used for data backup and some high volume recording devices such as instrument and satellite recorders.[1] The Generation 4 Ultrium format LTO tape provides for up to 1.6 TB in a single cartridge, with a compressed data transfer rate of up to 320 MB/s.[2] The high volumetric density is achieved by a combination of high areal density and the use of a thin tape. This requires that the substrate and tape be mechanically and environmentally stable in both the longitudinal (for high linear density) and lateral (for high track density) directions. For high track density, the lateral tape motion and track spacing variation arising from dimensional changes of the tape must be controlled for low drive error performance.[3] Controlling the track spacing requires a better understanding of the dimensional stability of the tape, especially of the polymeric substrate that takes 75 to 95% of the total thickness. Also, because the high coercivity magnetic film on metal evaporated tape is deposited and heat treated at elevated temperature, a substrate with stable mechanical properties up to a temperature of 100–150°C or even higher is desirable.[1] One of the key concerns to tape and substrate manufacturers is the degradation of the substrate during tape manufacturing, which has not been previously reported.

The second author's group has extensively studied the viscoelastic properties and dimensional stability of ultrathin polymeric films and tapes.[1,4–9] This includes the creep, shrinkage, and dynamic behavior analysis of polymeric substrates, tapes, and stripped tapes (without back coating). Weick and Bhushan[8,9] modeled the magnetic tape as a three-layer composite: front layer, substrate, and back coat. By applying the rule of mixtures, the viscoelastic behavior of each individual layer was obtained, and the strain distribution was predicted through the thickness of the tape.

*Correspondence to:* B. Bhushan (bhushan.2@osu.edu).

Contract grant sponsor: Nanotribology Laboratory for Information Storage, The Ohio State University.

Contract grant sponsor: MEMS/NEMS (NLIM), The Ohio State University.

Journal of Applied Polymer Science, Vol. 88, 2082–2096 (2003)
© 2003 Wiley Periodicals, Inc.

Even with the great amount of work done on the reliability of magnetic tape and substrate, measurements of important properties such as Poisson's ratio, lateral creep behavior, and thermal expansion of individual layers have not yet been reported. The difficulty of measuring the Poisson's ratio stems from the fact that the polymer films are thin membranes, thus making it very difficult to attach strain gauges to the sample. Furthermore, the chemical sensitivity and highly nonequilibrium molecular structure limit the use of printing/marking on these films.

A precise noncontact measurement technique based on the use of a laser scan micrometer (LSM) was developed by the authors to measure the lateral deformation behavior of thin polymer films.[10] In this study, the so-called profile-matching technique was improved to study the lateral deformation of magnetic tapes and its layers. Two metal particle (MP) tapes and two metal evaporated (ME) tapes, each of which use two typical polyester substrates, polyethylene terephthalate (PET) and polyethylene naphthalate (PEN), were studied. Selected layers were removed by suitable procedure to obtain the stripped tape samples. The lateral deformation behavior and Poisson's ratio of the magnetic tapes and stripped layers were measured. The properties of the never-coated raw film and the substrate after stripping coatings from the tape were compared, and the degradation of the substrates during tape manufacturing was discussed. To study the behavior of the tapes during storage, the lateral creep of the various samples was measured. The thermal and hygroscopic expansions of the above samples were also measured, and the thermal expansion data were compared with that measured by thermal mechanical analysis (TMA).

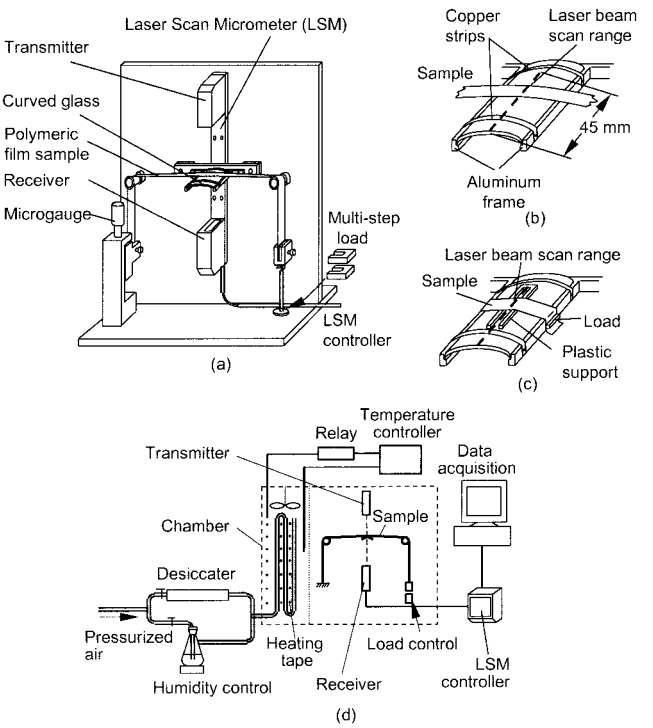


**Figure 1** Schematic of (a) lateral profile measurement apparatus, (b) details of the curved glass for lateral profile measurement, (c) details of the curved glass with a plastic support for thermal/hygroscopic expansion measurements, and (d) functional block diagram of the measurement system.

## EXPERIMENTAL

### Apparatus and procedure

#### Poisson's ratio and short-term lateral behavior

Figure 1(a) shows the schematic diagram of the experimental apparatus developed to conduct the Poisson's ratio measurement. An opaque sample, 280 mm long and 12.7 mm wide, was loaded at one end, and fixed to a microgauge at the other end. The laser scan micrometer (LSM) system (transmitter, LS5041T; receiver, LS5041R; and controller, LS5501; Keyence Corp., Osaka, Japan), with a measurement accuracy of 2 $\mu$m and a resolution of 0.05 $\mu$m, was used to measure the width of the sample. Figure 1(b) shows details of the measurement area. A curved quartz glass (85 mm radius) was used to support the polymeric sample and prevent it from puckering in the transverse direction under a longitudinal stress. To achieve this, the sample should have good contact with the curved glass, at least at the measurement point. On the other hand, the polymer film tends to stick to the curved glass, especially when the humidity is high. This induces extra static friction force and prevents the uniform distribution of the stress over the length of the sample. In this work, the sample maintained a "line" contact with the curved glass by controlling the contact angle at approximately 3–5°.

The experimental apparatus was placed inside a chamber [Fig. 1(d)], where temperature and relative humidity were controlled at 25 $\pm$ 0.5°C and 50 $\pm$ 2%RH, respectively. Airflow inside the chamber was also controlled so that air did not blow directly on the sample while maintaining uniform environmental conditions inside the chamber. The sample was preloaded to a normal load of 0.5 MPa. After the temperature and humidity reached the desired values, the sample was conditioned for another 30 min before the test was started. Calibration tests showed that, under a stress of 0.5 MPa, the lateral dimensional change of the sample after 30 min for a period of 20 h was within 0.2 $\mu$m, less than 0.0016% lateral strain. Therefore the samples may be regarded as having reached equilibrium after 30 min of conditioning.

The LSM was composed of various materials that change dimension according to the environmental condition. The scanning position of the laser beam was determined by the refractive index of the atmosphere

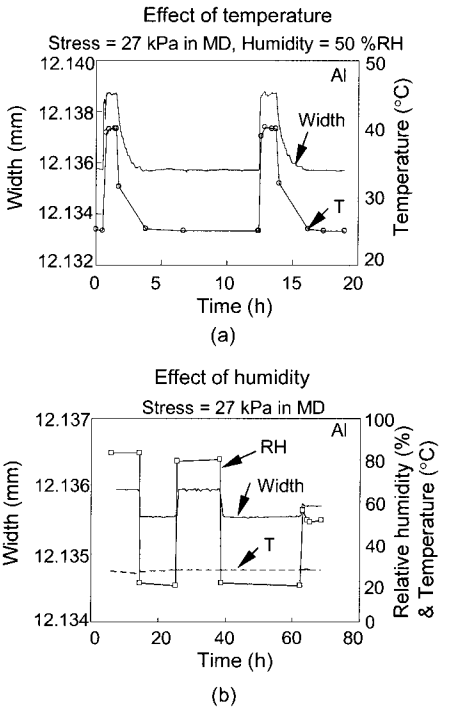


**Figure 2** Effect of (a) temperature and (b) relative humidity on the width change of Al foil sample for calibration of the test apparatus. T, temperature; RH, relative humidity.

and lens, which is also affected by the temperature and humidity. In this work, a 15.4 $\mu$m thick aluminum foil (Reynolds, Columbus, OH) sample was used to calibrate the systematic error. The foil was slit to about 12.1 mm width. Figure 2 shows the measurement results of the width of the Al sample affected by the change of temperature and humidity. The CTE of Al foil is known to be $23.6 \times 10^{-6}$/°C for 25–50°C. Thus a 12.1-mm sample should expand 4.3 $\mu$m from 25 to 40°C. The measurement shows a 3.1 $\pm$ 0.1 $\mu$m expansion, so there is a $-1.2$ $\mu$m systematic error. To confirm that systematic error is the same for various samples and to determine the accuracy of the measurement, the thermal expansion of a standard polycrystalline alumina (99.5%) rod sample (10 mm diameter) was measured at the same conditions: 25 to 40°C, while the humidity remained constant at 50%RH. A support was used to hold the rod sample over the curved glass. The measured expansion was $-0.5 \pm 0.1$ $\mu$m, whereas the theoretical value should be 0.7 $\mu$m. Thus the systematic error of the LSM was confirmed as $-1.2$ $\mu$m when the temperature changed from 25 to 40°C and the relative humidity was maintained constant at 50%. This systematic error was also confirmed by the manufacturer. The accuracy and repeatability in the width change was established to be $\pm 0.1$ $\mu$m from these tests on aluminum and alumina samples. Similarly, the LSM has a systematic error of about 0.4 $\mu$m when the relative humidity changes from 15 to 80%RH at 25°C (Fig. 2). These errors were subtracted out in the experiments when the measurements for different conditions were compared. The measured fluctuation at a given condition is about $\pm 0.1$ $\mu$m, as indicated in Figure 2. This is taken to be the resolution of the apparatus when the dimensional changes are measured at constant environmental conditions, such as during the measurement of lateral deformation behavior and Poisson's ratio.

For the measurement of Poisson's ratio, the sample was loaded in steps over a load range, say from 5 to 42 MPa, at a step interval of 7 MPa. At each load level, the sample was held for 12 min to stabilize the measurement. The width profile was measured by moving the sample in the longitudinal direction at a speed of 10 $\mu$m/s [for an example, see Fig. 3(a)]. By comparing the profiles at different load levels and matching the position of the characterized features, the lateral and longitudinal displacements of the sample at the corresponding stress were obtained. Thus the longitudinal and lateral deformation and Poisson's ratio were calculated.

$$\nu = \frac{\varepsilon_{\perp}}{\varepsilon_{\parallel}} = \frac{\Delta w/w}{\Delta l/l} = \frac{\Delta w l}{\Delta l w} \tag{1}$$

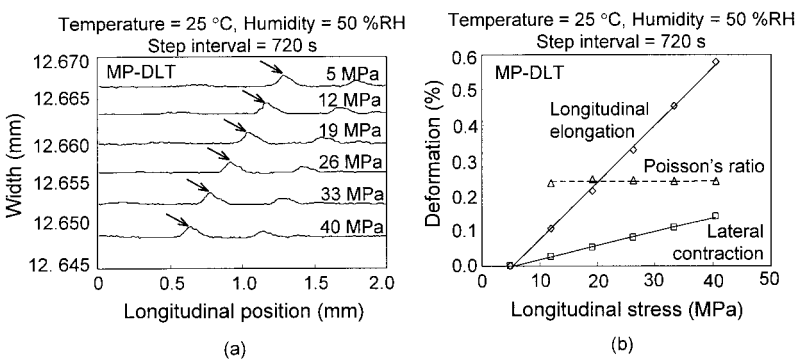


**Figure 3** (a) Width profiles of MP-DLT tape at various stresses; arrows indicate a typical feature in the profile. Profile matching, by calculating the shifting of a feature, is used to obtain (b) longitudinal elongation, lateral contraction, and Poisson's ratio.

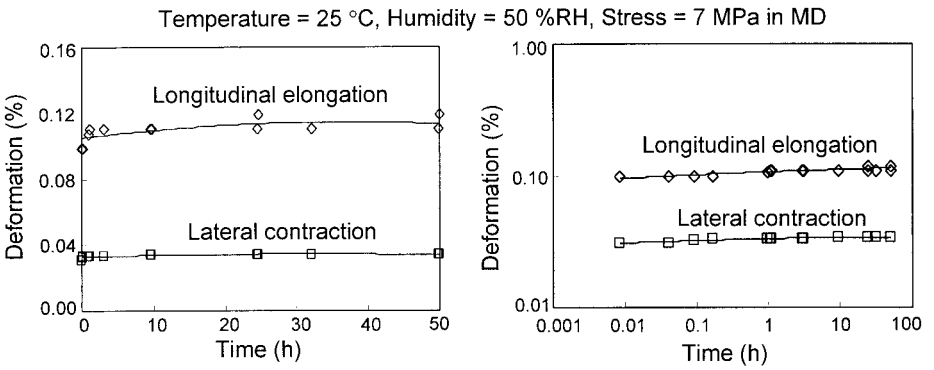


**Figure 4** Longitudinal elongation and lateral contraction of T-PET(2) film.

where $\nu$ is the Poisson's ratio; $\epsilon_{\perp}$ is the lateral contraction; $\epsilon_{\parallel}$ is the longitudinal elongation; $w$ is the sample width; $\Delta w$ is the decrease of the width; $l$ is the sample length from the microgauge to the measuring point; and $\Delta l$ is the increase of the length. Figure 3(b) shows the longitudinal elongation, lateral contraction, and corresponding Poisson's ratio for MP-DLT tape (to be described later) at 25°C, 50%RH. The results show a good linear relationship.

## Long-term lateral creep behavior

For measurement of long-term creep behavior, the sample was conditioned at 0.5 MPa for 1 h, and loaded at another 7 MPa for 50 h. In the previous work,[10] the long-term creep behavior was measured by way of equal loading, not by the so-called profile matching. That is, the sample was loaded equally on both ends, and the width of the sample was measured at the center of the sample. The advantage is that continuous data can be obtained; the disadvantage is that only the lateral deformation is measured, and also if the sample moves during the period, the test fails. The experimental results show that, even though the loads and the environmental conditions were strictly controlled, the sample still had a chance to move during the 50-h test. Although the movement was on the microscale, it could spoil the test, given that the edge of sample was not smooth. Thus in this study, the long-term creep behavior was measured by loading the sample at one end, as shown in Figure 1(a), and the width profiles were measured at various time periods. Thus, the lateral contraction and longitudinal elongation at various times were recorded. This improved technique has proved to yield stable and reliable results. Figure 4(a) and (b) show typical long-term deformation of T-PET(2) (to be described later) raw film.

## Coefficient of thermal expansion (CTE) and coefficient of hygroscopic expansion (CHE)

Figure 1(c) shows the details of the sample and curved glass, set for CHE measurements. A sample (42 mm long; 12.7 mm wide) was slightly loaded in the machine direction (MD). The dimension in the transverse direction (TD) of the sample was measured as the humidity changed from 15 to 80%RH, whereas the temperature was controlled at 25 ± 0.5°C; the CHE in TD was thus obtained. The load was about 50 kPa, within the range recommended by ASTM E831-93 and D696-98 standards.[11] The load did not result in significant creep of the sample during the test. Two hygroscopic cycles were carried out on each sample.

The apparatus was also used to measure the CTE. However, the variable temperature range limited by the LSM was from ambient to 45°C. Over such a small temperature range, the measuring error should be large, and does not provide reliable data. Instead, a commercially available standard thermomechanical analyzer (TMA) (TA2940; TA Instruments, New Castle, DE) is commonly used and was used in this study to measure CTE.

Figure 5 shows a schematic diagram of the TMA setup for the film sample measurement. The sample was mounted between a static stage and a floating probe. The temperature and heating speed were controlled by two thermocouples placed close to the sam-

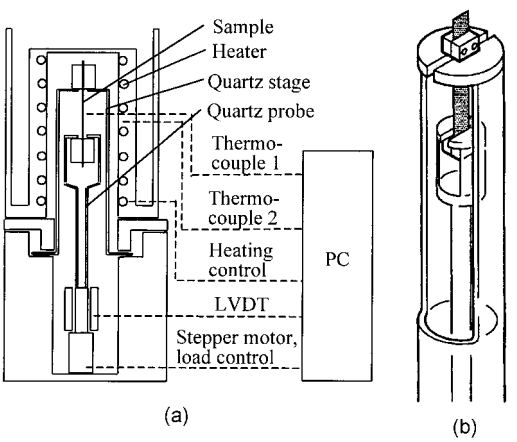


**Figure 5** Schematic diagram of thermal mechanical analysis (TMA) instrument.

ple and inside the heater. The dimensional change of the sample was recorded by the LVDT. The force applied on the sample was controlled by the stepper motor and corresponding load control. The typical sample size in this study was 3 × 40 mm; after clipping, the gauge length of the sample was approximately 25.5 mm. For the samples cut in the TD of tapes, the sample length was 12.67 mm, and the gauge length was about 8.7 mm. The temperature ranged from 10°C (precooled) to 70°C, at a heating rate of 3°C/min. A constant 3 g force was applied to the sample to keep it flat.

After the dimensional change of the sample was measured, it was converted to the CTE as

$$\alpha = \frac{\Delta l}{l \Delta T} \tag{2}$$

where $\Delta l$ and $l$ are length change and the original length at 10°C, respectively; and $\Delta T$ is the temperature range. According to ASTM E831-93, the measured CTE during the first 20°C of the test (10–30°C) was regarded as unstable, and was not used in the discussion in this study. The data were then converted by replacing the original length in eq. (2) to the length at 30°C, so that the data would coincide with zero expansion at 30°C. Aluminum foil (15.4 μm thick; Reynolds; CTE = $23.6 \times 10^{-6}$/°C) was used to calibrate the instrument. The results of three repeated tests on this foil were 23.6, 23.4, and $23.6 \times 10^{-6}$/°C, so the TMA was proved to have good repeatability.

## Samples

Magnetic tapes selected for this study are shown in Figure 6(a) and (b). These tapes are representative of the two basic types of magnetic tapes, MP tapes in which magnetic particles are dispersed in a polymeric binder; and ME tapes in which continuous films of magnetic materials are deposited on to the substrate using vacuum techniques. Both of the MP tapes in this study (MP-DLT and MP-LTO) had a 6.1 μm thick substrate (either PET or PEN), an approximately 2.3 μm thick front coat (including magnetic and nonmagnetic layers), and an approximately 0.5 μm thick back coat. The ME tapes (ME-Hi8 and ME-MDV) also had an approximately 0.5 μm thick back coat and an approximately 0.13 μm thick front coat. The substrate of ME-Hi8 was 9.9 μm thick PET, and that for ME-MDV was 4.7 μm thick PEN.

PET and PEN films have been widely studied.[1,7,12] The glass-transition temperatures of the PET and PEN substrate are 70–80 and 120°C, respectively.[7,12] Information about the specific chemistry of the materials used in the front coats and back coats was not available from the manufacturers. However, based on Bhushan,[1] the front coat may consist of a single magnetic layer, as in the cases of single-layer MP tapes. Their composite magnetic layer consists of magnetic particles, a polymer binder, lubricant, abrasive (mostly alumina), and conductive carbon particles. The front coat may also consist of a magnetic layer and a nonmagnetic polymer underlayer, as in the case of double-layer MP tape. For ME tapes, the front coat consists of a magnetic layer, a DLC coating, and a lubricant layer. The ME tape magnetic layer is a continuous thin film of Co—Ni—O deposited by evaporation. The back coat consists of carbon black in a polymeric binder.

The symbols and thickness of the detail samples are listed in Table I. They include the following layer formats:

Magnetic tapes as cut from the cassettes
Substrates (front coat and back coat removed) (S)
Substrate plus front coat (back coat removed) (SF)
Substrate plus back coat (front coat removed) (SB)
Never-coated raw substrate film

To obtain the substrate for the MP tapes, methyl ethyl ketone (MEK) was used to remove the front coat and back coat. This involved placing the tape on a flat piece of glass and rubbing both sides of the tape longitudinally with a paper towel saturated with MEK until only the transparent PET substrate remained. The substrate for the ME tape was obtained in a similar manner. However, MEK could be used to remove only the back coat of the ME tape. A 2% hydrochloric acid solution was used to remove the front coat. This procedure involved dipping the ME tape into the solution until the metal-evaporated coating could be rubbed off.

Removing the back coat of the MP and ME tapes without removing the front coat involved spreading a thin bead of distilled water on a glass plate. The tape specimen was then placed front coat down in this bead of water. All excess water around the edges of the tape was soaked up with a paper towel. The back coat could then be carefully removed using MEK, and the thin film of polar water molecules between the glass plate and front coat of the tape helped prevent the nonpolar MEK molecules from dissolving the front coat. Removing the front coat on the MP and ME tapes without removing the back coat involved a similar procedure.

The substrates and raw films were sputter coated with gold to make them opaque and capable of being measured by LSM. All the samples were left in ambient condition (22–24°C, 30–60%RH) for at least 4 days before testing.

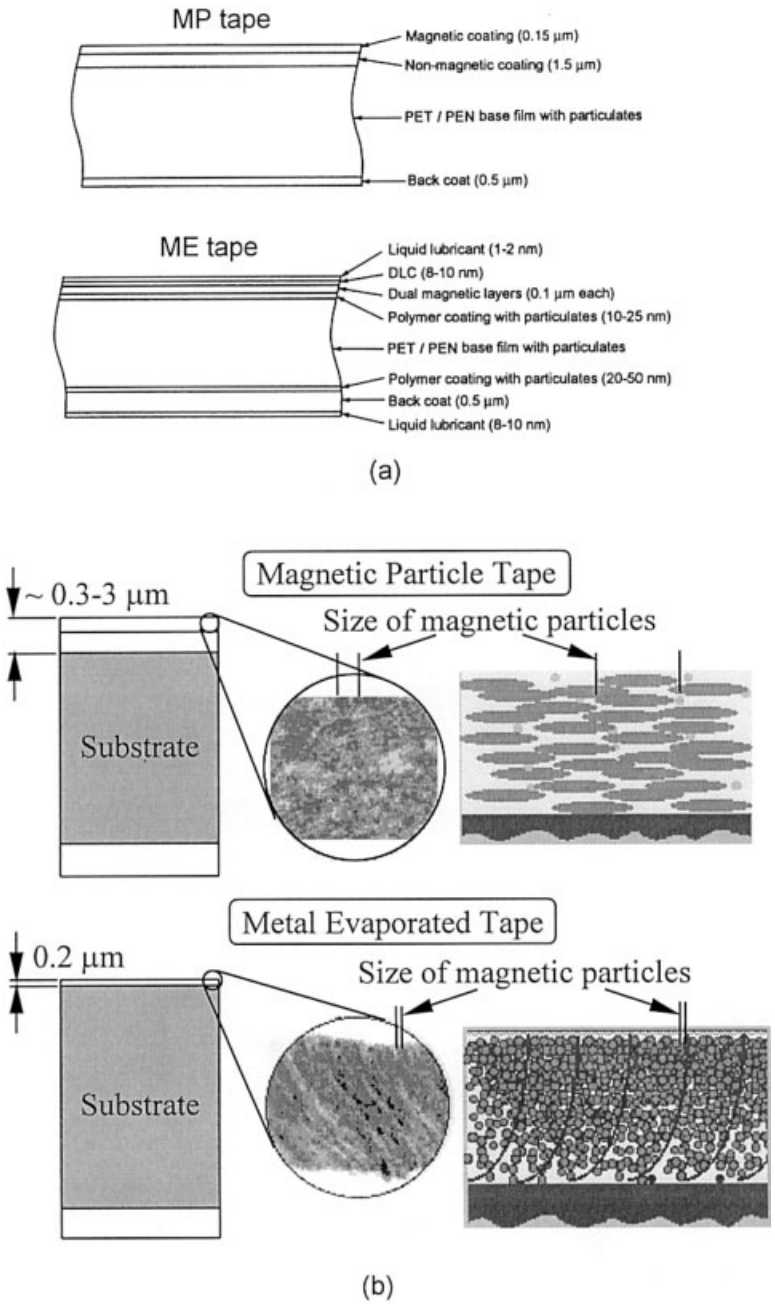


**Figure 6** (a) Schematic diagram of MP and ME tapes; (b) detailed construction of MP and ME tapes. (Downloaded from http://www.sony.co.jp/en/Products/METape/eng/why/index.html, and slightly modified.)

### Rule of mixtures approach

Because magnetic tapes consist of multiple layers, they resemble polymer composite laminates. Generally, they can be regarded as a three-layer composite, as shown in Figure 7. The rule of mixtures method can be used to predict the elastic modulus, which corresponds to the longitudinal elongation in this study, of the whole tape if the data for each layer are known, assuming that there is perfect bonding between each layer, that is, assuming isostrain.[13]

$$\sigma_t A_t = \sigma_f A_f + \sigma_s A_s + \sigma_b A_b \tag{3}$$

where $\sigma_t$, $\sigma_f$, $\sigma_s$, and $\sigma_b$ are the stresses in the entire tape, front coat, substrate, and back coat, respectively; and $A_t$, $A_f$, $A_s$, and $A_b$ are the cross-sectional areas of the tape, front coat, substrate, and back coat, respectively. Also,

$$E_t t = E_f f + E_s s + E_b b \tag{4}$$

where $E_t$, $E_f$, $E_s$, and $E_s$ are the Young's moduli of the tape, front coat, substrate, and back coat, respectively; and $t$, $f$, $s$, and $b$ are the thicknesses of the corresponding layers. All the mechanical properties correspond

**TABLE I**
**Sample Matrix: Symbols and Thickness ($\mu$m)**

| Tape | Width (mm) | Substrate + front coat | Substrate + back coat | Substrate | Never coated substrate film[a] |
|---|---|---|---|---|---|
| MP-DLT 8.9 | 12.67 | MP-DLT/SF ~ 8.4 | MP-DLT/SB ~ 6.6 | MP-DLT/S 6.1 | T-PET(2) 6.1 |
| MP-LTO 8.9 | 12.67 | | | MP-LTO/S 6.1 | T-PEN 6.1 |
| ME-Hi8 10.66 | 8 | ME-Hi8/SF ~ 10.13 | ME-Hi8/SB ~ 10.43 | ME-Hi8/S 9.9 | T-PET(3) 9.9 |
| ME-MDV 5.36 | 6.35 | | | ME-MDV/S 4.7 | T-PEN(2) 4.7 |

[a] T-PEN corresponds to the sample in Bhushan et al.[7] T-PEN(2), T-PET(2), and T-PET(3) are new samples.

to the loading direction, that is, the longitudinal direction.

For any two combined layers, similar equations apply, such as

$$E_{fs}(f + s) = E_f f + E_s s \tag{5}$$

where $E_{fs}$ is the Young's modulus of the combined layers of substrate plus front coat.

Because we know two of the moduli in eq. (5), for example, $E_{fs}$ and $E_s$, and the thickness of each layer, we can calculate the third modulus.

To calculate the Poisson's ratio and lateral contraction of the individual layers from the data of the substrate and combined layers, a modified model was developed and is presented in the appendix. The model is based on isostrain in the longitudinal direction, and requires the Young's moduli of the combined layers in TD. These data are currently not available. The model for calculating the thermal expansion of individual layers is also presented in the appendix. However, the model cannot be used to obtain data for various layers because high temperature Young's moduli data are not known.

## MECHANICAL BEHAVIOR OF THE VARIOUS LAYERS OF MAGNETIC TAPES

### Poisson's ratio and lateral and longitudinal deformation properties

Table II lists the Poisson's ratio, lateral and longitudinal deformations, and the Young's modulus in the longitudinal direction. It should be noted that the "Poisson's ratio" is the average value over a stress range of 5 to 42 MPa, whereas the "lateral contraction" and "longitudinal elongation" indicate the deformation at 7 MPa. Therefore the Poisson's ratio may not be exactly equal to the ratio of lateral contraction over longitudinal elongation in that table.

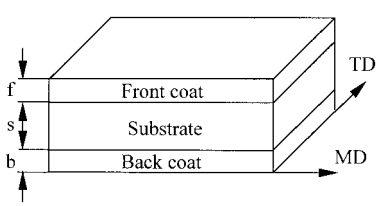


**Figure 7** Nomenclature used for rule of mixtures equations.

Generally, ME tapes show lower lateral contraction and lower Poisson's ratio than MP tapes. Although the Young's moduli of the substrates in the MD direction of MP tapes are higher than those of ME tapes, the Young's moduli of the final MP tapes and ME tapes are close.

From the data in Table II, the mechanical properties of the MP tapes are more influenced by the substrate film than are ME tapes. The Young's moduli of SF (6.48 GPa) and SB (6.60 GPa) of MP-DLT are slightly lower than that of the substrate (6.93 GPa), which means both the front coat and back coat are less stiff than the substrate in MD. By comparing the MP-DLT and MP-LTO, it is clear that the high Young's modulus substrate results in a high Young's modulus tape. This tendency is not clear for ME tapes. Both the ME-Hi8 and ME-MDV tapes show similar Young's moduli and lateral deformation behavior. The mechanical properties of the front coat are dominant, given that the Young's modulus of SF (4.93 GPa) of ME-Hi8 is significantly higher than that of SB (3.87 GPa) and substrate (3.63 GPa). In this case, both the front coat and back coat are stiffer than the substrate in MD.

Poisson's ratio and lateral contraction information for individual layers are not available for the reason stated earlier. However, we can use the rule of mixtures to obtain longitudinal Young's modulus data for individual layers of MP-DLT and ME-Hi8 tapes. The calculation results are listed in Table III; they include the data for both front and back coats for MP-DLT tape and ME-Hi8 tape. To validate the procedure, eq. (4) was used to calculate values of the three-layer composite (tape). These data are also listed in Table III, and compared with the data for the measured data of the magnetic tapes. The results show good agreement.

In Table III, the Young's moduli for the composition layers of MP-DLT tape are of the same order of magnitude, ranging from 2.6 to 6.9 GPa. This means that the mechanical properties of the magnetic layer are primarily determined by the polymer binder, and not by the embedded particles. In ME-Hi8 tape, the Young's modulus of the front coat is about 10 times higher than that of other two layers; for example, 62

**TABLE II**
**Experimental Data of Poisson's Ratio and Lateral and Longitudinal Deformation Properties of the Tape Samples[a]**

| Tape sample | Poisson's ratio[b] | Lateral contraction at 7 MPa (%) | Longitudinal elongation at 7 MPa (%) | Young's modulus (GPa) |
|---|---|---|---|---|
| MP-DLT | 0.24 | 0.027 | 0.117 | 5.98 |
| MP-DLT/SF | 0.23 | 0.026 | 0.108 | 6.48 |
| MP-DLT/SB | 0.32 | 0.032 | 0.106 | 6.60 |
| MP-DLT/S | 0.34 | 0.036 | 0.101 | 6.93 |
| T-PET(2) | 0.32 | 0.033 | 0.099 | 7.07 |
| MP-LTO | 0.29 | 0.037 | 0.145 | 4.83 |
| MP-LTO/S | 0.37 | 0.045 | 0.137 | 5.11 |
| T-PEN | 0.38 | 0.047 | 0.133 | 5.26 |
| ME-Hi8 | 0.20 | 0.028 | 0.138 | 5.07 |
| ME-Hi8/SF | 0.19 | 0.027 | 0.142 | 4.93 |
| ME-Hi8/SB | 0.21 | 0.033 | 0.181 | 3.87 |
| ME-Hi8/S | 0.21 | 0.042 | 0.193 | 3.63 |
| T-PET(3) | 0.21 | 0.035 | 0.174 | 4.02 |
| ME-MDV | 0.20 | 0.024 | 0.134 | 5.22 |
| ME-MDV/S | 0.19 | 0.035 | 0.173 | 4.05 |
| T-PEN(2) | 0.23 | 0.039 | 0.191 | 3.66 |

[a] All data were measured at 25 ± 0.5°C, 50 ± 1% RH.
[b] Poisson's ratio was measured at a stress range of 5 to 40 MPa, stress step of 7 MPa, and time interval of 12 min.

GPa for the front coat and 3.6 GPa for the substrate. Although the thickness is limited, the DLC and evaporated magnetic layer greatly stiffen the tape. According to the rule of mixtures, or the isostrain assumption, the load on the tape is mainly taken by the front coat, which is mechanically stiffer than the substrate.

It is interesting to note that the substrates for ME tapes have low Poisson's ratios, and are very close to the Poisson's ratio of the final tape. Tape manufacturers probably selected the substrate so that there is less strain mismatch between the substrate and ME front coats.

As shown in Table II, the longitudinal elongation of the substrate films varies significantly but the difference among their lateral contractions is not significant. This reflects a clear difference in the Poisson's ratios.

**TABLE III**
**Calculated Young's Modulus of MP and ME Tapes and Coatings**

| Sample | Young's modulus (GPa) |
|---|---|
| MP-DLT/S (measured) | 6.93 |
| MP-DLT/F (calculated) | 5.29 |
| MP-DLT/B (calculated) | 2.62 |
| MP-DLT (calculated) | 6.26 |
| MP-DLT (measured) | 5.98 |
| ME-Hi8/S (measured) | 3.63 |
| ME-Hi8/F (calculated) | 62.5 |
| ME-Hi8/B (calculated) | 8.63 |
| ME-Hi8 (calculated) | 5.07 |
| ME-Hi8 (measured) | 5.14 |

### Degradation of substrates after tape manufacturing

In Table II, we compare the degradation of the substrate after tape manufacturing. For longitudinal elongation, both T-PET(2) and T-PEN show slight degradation from the raw film to the stripped substrates of MP tapes; the change is within a couple of percent. However, the case is dramatically different for ME tapes. The T-PET(3) shows a 10% degradation after tape processing, whereas T-PEN(2) shows a 10% enhancement after processing. The phenomena are also shown by lateral contractions data. The changes before and after MP tape processing are minor, but those after ME tape processing are significantly different for PET and PEN substrates. The lateral contraction of T-PET(3) (ME-Hi8 substrate) increases from 0.035 to 0.042%, whereas that of T-PEN(2) (ME-MDV substrate) decreases from 0.039 to 0.035%.

To get a clear comparison of the degradation mechanisms of PET and PEN films after tape manufacturing, 50-h lateral creep behavior was studied for the four substrates and corresponding raw films, results of which are shown in Figure 8. The small windows in the T-PET(2) and T-PEN figures show repeated data from short-term tests. The data for the raw film are more scattered than are data for the stripped substrate, but the tendency is clear. The PET films show clear degradation after tape manufacturing, whereas PEN films are more stable, or even enhanced.

In typical MP tape manufacturing,[1] substrate processing includes UV treatment, a driving stress up to

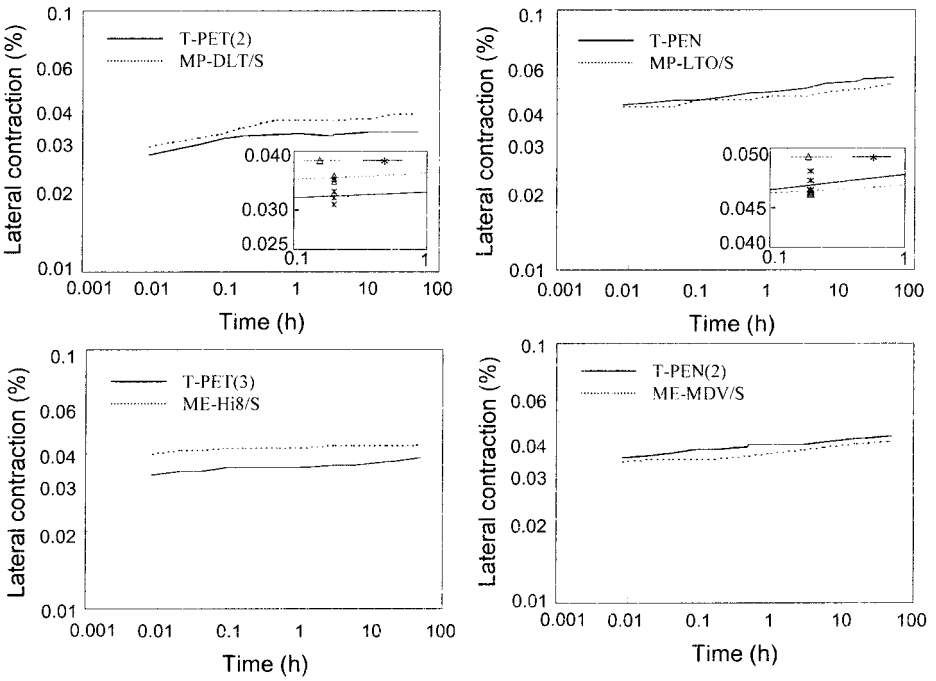


**Figure 8** Degradation of substrates after tape manufacturing.

30 MPa, drying at 50–80°C, and calendaring at 60–100 MPa and 60–80°C. There is no direct measurement of the temperature the substrate experiences during ME tape manufacturing because it quickly rotates with a water-cooled copper drum during the metal evaporating. Because the metallic vapor of the coating material can be more than 1000°C, it is reasonable to infer that the substrate experiences much higher temperature exposure in ME tape than in MP tape manufacturing.

As generally reported, the glass-transition temperature ($T_g$) of PET film is about 70 to 80°C. MP tape manufacturing is close to this threshold value, and the processing of ME tape could be higher than that, although only for a short period. The $T_g$ of PEN films is reportedly 120°C; thus, PEN is more thermally stable than PET because of the rigid naphthalene ring in its molecular structure.

Studies have shown that the annealing below the $T_g$ does not result in a significant decrease in mechanical properties.[1,14,15] Instead, annealed PEN films were found to have a lower loss tangent (tan $\delta$) at the $\alpha$-relaxation, and a lower decrease in relaxation moduli (moduli at very low deformation frequencies).

Gillmor found that the annealing treatment influences the $\alpha$-relaxation only.[16] The viscoelastic properties of PEN films at ambient temperatures are controlled by the $\beta^*$ process, that is, a secondary relaxation over 30 to 70°C.[7,17] All the substrate films used in this study were biaxially oriented, and were metastable in two respects. First, the percentage crystallinity of the film is much lower than the equilibrium crystalline content. Second, amorphous regions of the film contain frozen-in strains that tend to relax and allow the film to contract.[1] By combining these aspects, we can explain why PEN films do not show significant degradation (they actually show some enhancement) after tape manufacturing. The typical crystallinity of PEN film was reportedly about 30–40% (that of PET films is about 40–50%). It thus has a relatively large driving force to crystallize during thermal exposure.

When the temperature is higher than the glass-transition temperature, the main chain of the polymer film molecules will have enough energy to move and rotate. As a result, the biaxially oriented structure could be significantly affected. The mechanisms of thermal degradation include the residual stress relaxation, molecule segments recoiling, and selected chain scission or random chain scission.[18] The strength in the amorphous region is thus weakened. This effect is, obviously, more significant for the mechanical properties along the direction with the higher stretch ratio. Because the MP-DLT tapes in this study are used for linear drives, the substrates [T-PET(2)] are more stretched in MD than TD. That is why the stiffness of the MP-LDT/S in MD is more degraded than in TD after tape manufacturing.

Because the mechanical properties of both PET and PEN films change much more after ME tape processing than after MP tape processing, we can conclude that the substrates undergo higher temperature exposure in ME processing than in MP processing.

### Long-term lateral creep behavior of various layers of tape samples

Figure 9 shows the lateral creep of the various layers of the tapes, on both a linear scale and a log–log scale. Based on the data of the substrate and combined lay-

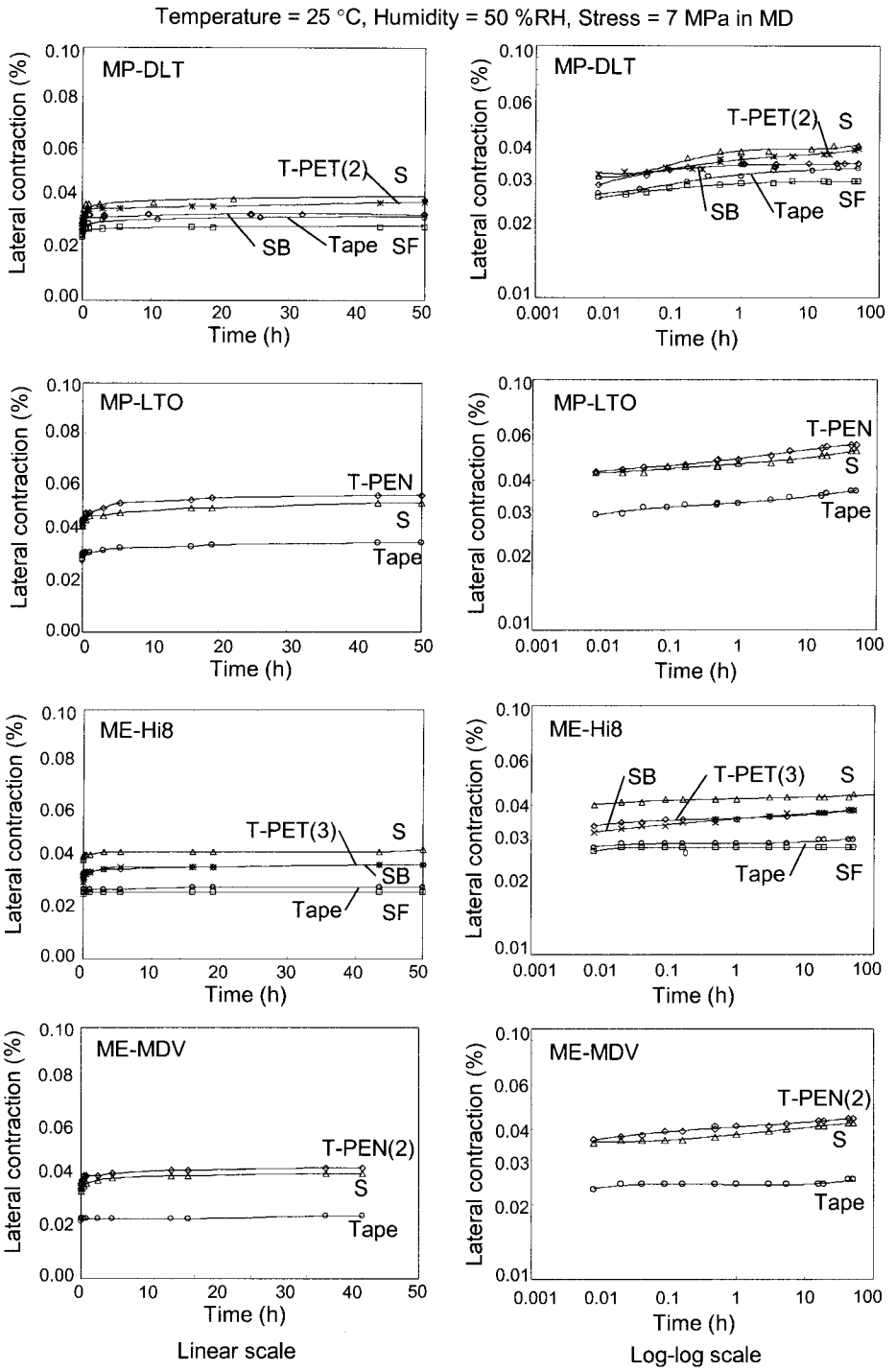


**Figure 9** Lateral creep of tapes and tapes with some of the layers removed.

ers (SF and SB), a model was developed to calculate the lateral creep of the individual layers of the magnetic tapes (shown in the appendix). Unfortunately, we need Young's moduli data for the tape samples (including combined layers SF and SB) in TD, and they are not available in this study because of the sample size. Theoretically, these moduli can be obtained from the tape web before it is slit.

## THERMAL AND HYGROSCOPIC EXPANSION PROPERTIES OF THE VARIOUS LAYERS OF MAGNETIC TAPES

One of the most important properties of magnetic tape is its thermal stability. One goal is to match the thermal expansion of the tape in TD, for linear tape drive application, to that of the head substrate ($\sim 7 \times 10^{-6}$/

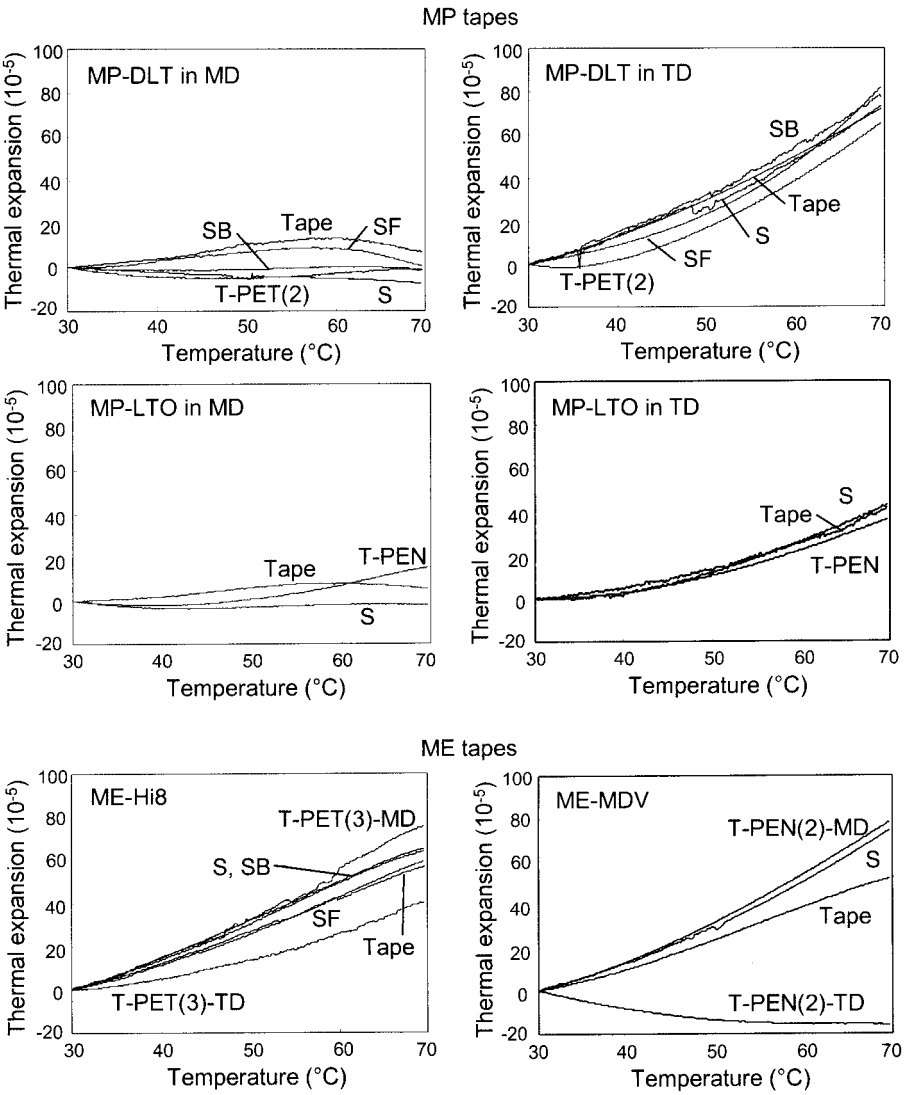


**Figure 10** Thermal expansion curves as a function of temperature for various samples.

°C[4]). If the tape has a significantly different value for CTE, it would be difficult for the head to locate the written tracks in the tape when the temperature changes. Thermal expansion behavior also gives some information about the molecular structure of a polymer substrate. As mentioned previously, the biaxially oriented films tend to recrystallize and release the residual stress/strain built up during manufacture of the film. Both of these factors result in shrinkage of films at elevated temperature. Some laboratory work showed that for PEN films, an increased stretch ratio in MD results in a higher Young's modulus and lower CTE in this direction.[19]

Thermal expansion curves for the samples are shown in Figure 10. As explained earlier, all curves represent the expansions starting from 30°C and ending at 70°C. The corresponding CTE data are shown in Figure 11.

For MP-DLT samples, we can see a significant difference between the thermal expansion behavior along MD and TD. Because T-PET(2) film is developed for a linear tape substrate, the stretch ratio during the film manufacture is about 2.25 in MD → 3.6 in TD → 2.5 in MD,[20] and the Young's moduli from the tensile test are 8.0 GPa (MD) and 4.8 GPa (TD). The film is highly aligned in MD, and a high residual stress exists in this direction. At elevated temperatures, the residual stress is released. This results in shrinkage of the film. MP-DLT tape and SF layers show even more shrinkage in the thermal expansion curves, and the CTE of both becomes negative when the temperature is higher than 55°C. This means that the front coat contains more longitudinal residual stress/strain, and that it begins to be released at a temperature as low as 55°C. In TD, all the MP-DLT samples show similar thermal expansion character, and the CTE values are obviously

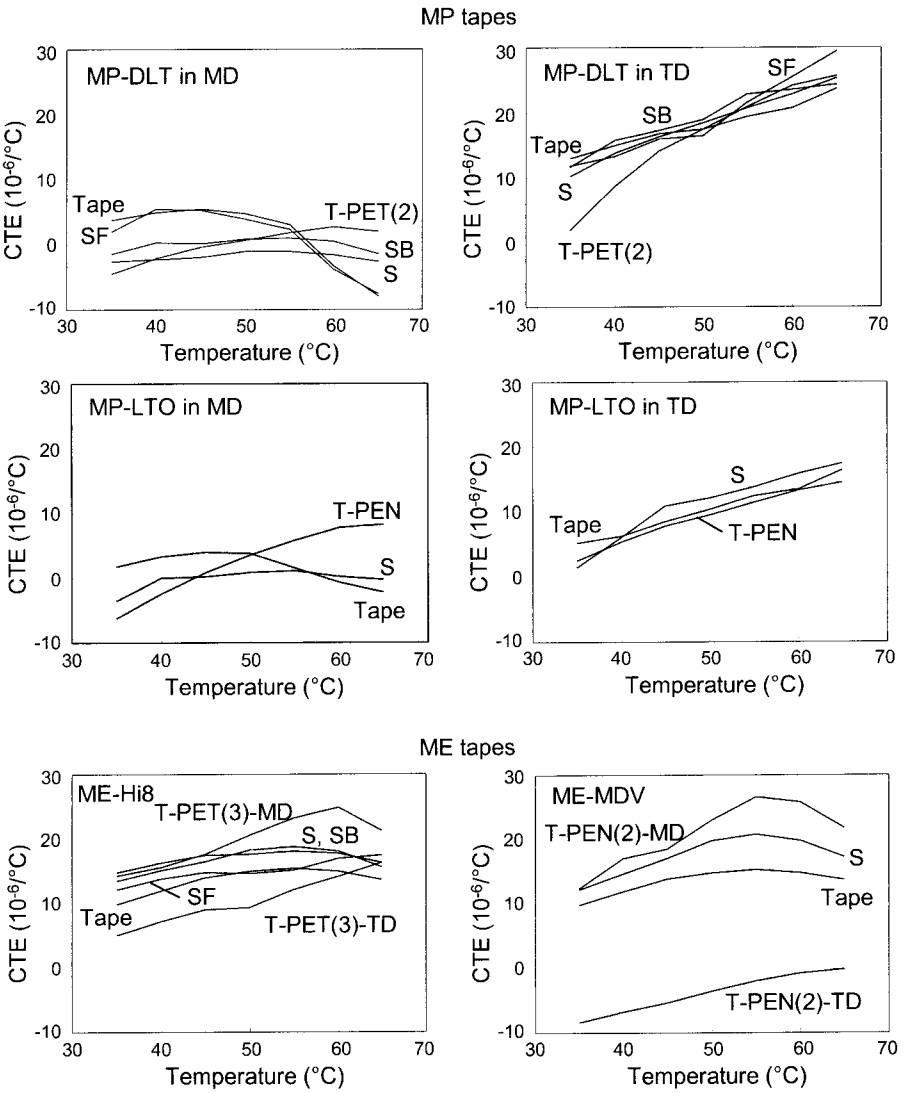


**Figure 11** Coefficient of thermal expansion as a function of temperature for various samples.

higher than those in MD. This comes from the fact that the films were not equally drawn.

By comparing the CTE data for stripped substrate and virgin film at elevated temperatures, we found that the CTE in MD decreased, and in TD slightly increased, after tape manufacturing. This tendency is present in all the substrates in this study. We believe this happens because the high driving force at elevated temperatures during tape manufacturing induces more residual strain in the machine direction, and it is not well annealed. The coating itself may also affect the mechanical properties of the substrate; that is, some compressive stress along MD remained between the coating and substrate after the coating process.

From Figures 10 and 11 it is clear that tapes and their respective substrates show similar thermal expansion. The CTEs of ME tape samples are obviously higher than those of MP tapes. Recall the Young's modulus of ME tape substrates in MD in Table II. They are also lower than those of MP tape substrates. The reason is that the ME tapes are used in helical scan drives, which require a higher stiffness in TD. Thus the substrate films for ME tapes are usually balanced, or TD oriented (MP tapes are MD oriented for high modulus in MD). As for ME-Hi8 samples, the CTE of the T-PET(3) in TD is slightly lower than that in MD. This implies that the Young's modulus in TD is higher than that in MD. For thin polymer films, lower CTE values usually result from a high stretch ratio and high stiffness in this direction. We do not have processing and mechanical data for T-PEN(2) from the manufacturer, but from the CTE data in Figure 11 we can conclude that T-PEN(2) films are highly oriented in TD, rather than in MD. In this study, all the polymer films show decreased CTE in MD after tape manufacturing, but they do not show any improvement in the stiffness in that direction. The reason is that thermal

**TABLE IV**
**Summary of the Coefficient of Thermal Expansion ($10^{-6}$/°C) Data Use TMA**

| Tape | Direction | Temperature range (°C) | | | |
|---|---|---|---|---|---|
| | | 30–40 | 40–50 | 50–60 | 60–70 |
| MP-DLT | MD | 3.8 | 5.6 | 3.1 | −7.9 |
| | TD | 12.9 | 16.8 | 19.5 | 23.8 |
| MP-DLT/SF | MD | 2.0 | 5.4 | 2.4 | −7.5 |
| | TD | 11.9 | 15.9 | 21.5 | 29.6 |
| MP-DLT/SB | MD | −1.3 | 0.2 | 1.1 | −1.4 |
| | TD | 11.7 | 17.3 | 22.9 | 24.3 |
| MP-DLT/S | MD | −2.6 | −1.9 | −1.1 | −2.5 |
| | TD | 12.6 | 16.2 | 22.3 | 26.2 |
| T-PET(2) | MD | −4.5 | −0.4 | 1.9 | 2.0 |
| | TD | 1.9 | 14.2 | 20.9 | 25.7 |
| MP-LTO | MD | 1.8 | 3.9 | 1.6 | −2.3 |
| | TD | 5.3 | 8.6 | 12.5 | 16.4 |
| MP-LTO/S | MD | −3.5 | 0.3 | 1.2 | −0.2 |
| | TD | 1.4 | 11.0 | 13.9 | 17.4 |
| T-PEN | MD | −6.3 | 0.9 | 5.8 | 8.3 |
| | TD | 2.5 | 7.8 | 11.5 | 14.6 |
| ME-Hi8 | MD | 9.9 | 13.9 | 15.4 | 13.7 |
| ME-Hi8/SF | MD | 12.1 | 14.8 | 15.2 | 17.4 |
| ME-Hi8/SB | MD | 14.8 | 17.4 | 18.1 | 16.2 |
| ME-Hi8/S | MD | 13.5 | 16.4 | 18.8 | 15.7 |
| T-PET(3) | MD | 14.3 | 17.6 | 23.3 | 21.2 |
| | TD | 5.1 | 8.9 | 12.2 | 16.3 |
| ME-MDV | MD | 9.9 | 13.8 | 15.4 | 13.7 |
| ME-MDV/S | MD | 12.3 | 17.1 | 20.8 | 17.3 |
| T-PEN(2) | MD | 12.4 | 18.6 | 26.6 | 21.8 |
| | TD | −8.4 | −5.3 | −1.9 | −0.2 |

degradation and residual stress are not sufficiently released after tape manufacturing.

The CTE data of the samples at various temperature ranges are also listed in Table IV. Based on the rule of mixtures, that is, the isostrain (in longitudinal direction) assumption, a model is proposed to calculate the CTE of the individual layers of magnetic tapes. To the best of our knowledge, the measurement of CTE of individual layers in magnetic tape has never been reported, although numerous thermal dynamic and heat transfer models were analyzed based on this measurement. (See the appendix for the model of CTE calculation.) Some data, like the Young's moduli of the combined layers at elevated temperature, are required; but we do not have them. The dynamic mechanical analysis (DMA) will be used in the future to obtain these data.

So far, there is not much work reported on the hygroscopic expansion data of the thin polymer films, although it is another important factor in magnetic media and other applications.[1,21] After all, the environmental relative humidity changes as dramatically as, if not more than, the temperature does. In our previous work, we reported measurement of the CTE and the coefficient of hygroscopic expansion (CHE) by the laser scan technique. Table V lists the data measured by this technique. The error of CTE is estimated to be about $\pm 1.5 \times 10^{-6}$/°C, whereas that for CHE is within $\pm 0.5 \times 10^{-6}$/%RH.

## CONCLUSIONS

A so-called profile matching technique was used to accurately measure the Poisson's ratio and both lateral and longitudinal deformation of thin polymeric films and magnetic tapes. The Poisson's ratios for MP-DLT and MP-LTO are 0.24 and 0.29, respectively, whereas those for both ME-Hi8 and ME-MDV are 0.20. The Poisson's ratios for substrate films in this study range from 0.21 to 0.38.

The rule of mixtures methodology was used to calculate the Young's modulus of the individual layers of MP and ME tapes, using the data for the substrate, substrate plus front coat, and substrate plus back coat.

**TABLE V**
**CTE and CHE Measured by the Laser Scan Technique**

| Tape | CTE[a] ($10^{-6}$/°C) | CHE[b] ($10^{-6}$/%RH) |
|---|---|---|
| MP-DLT | 10 | 10.9 |
| T-PET(2) | 16 | 13.0 |
| MP-LTO | 4 | 10.7 |
| T-PEN | 8 | 10.6 |
| ME-Hi8 | | 6.6 |
| T-PET(3) | | 8.9 |
| ME-MDV | | 6.9 |
| T-PEN(2) | | 3.0 |

[a] Condition: 50%RH, 25–40°C.
[b] Condition: 25°C, 15–80%RH.

A model based on the isostrain assumption was also developed to calculate the Poisson's ratio, lateral contraction, and thermal expansion behavior of the individual layers of the magnetic layer.

The degradation of the substrate results from high driving stress and, especially, the elevated temperature exposure during tape manufacturing. The effect is more obvious for the low glass-transition temperature $T_g$ substrate, given that the biaxially oriented molecular structure can be destroyed by the movement and rotation of main chain segments at temperatures higher than the $T_g$. The results in this work show that the PET substrates show 10 to 20% lateral stiffness loss after either MP or ME tape manufacturing. For the stiffness in the longitudinal direction, there is no significant decrease for PET substrate after MP tape processing. We think the driving stress helps to keep the molecules oriented in this direction and the temperature is not sufficiently high to result in rearrangement of the molecules. However, there is a clear decrease in longitudinal stiffness for PET substrates after ME tape processing, which is believed to be attributed to thermal degradation. The PEN substrates, on the other hand, show an enhancement of up to 10% in lateral and longitudinal stiffness after tape processing, the result of further crystallization at elevated temperatures.

The CTE data for the substrate film show a slight decrease in MD and increase in TD after tape manufacturing. In general, the tapes and their respective substrates show similar thermal expansion characteristics. In the machine direction, ME tapes have higher CTE than that of MP tapes. A model was developed to calculate the thermal expansion of the individual layers of the magnetic layer, although further DMA data are needed to obtain the final results.

The research reported here was supported by the industrial membership of Nanotribology Laboratory for Information Storage and MEMS/NEMS (NLIM) at The Ohio State University. The authors thank Hideaki Watanabe and Hirofumi Murooka (Teijin-DuPont Ltd. Japan) and Toshifumi Osawa (DuPont-Teijin Ltd.) for their generous support and samples [MP-DLT (Fuji), MP-LTO (IBM), ME-Hi8 (Sony), and ME-MiniDV (Panasonic)].

## APPENDIX

To calculate the Poisson's ratio and both the thermal and the hygroscopic expansion of the individual layer of magnetic tapes, the following assumptions are made:

- Ideal interface bonding: strain continuous across the interface (i.e., isostrain)
- Linear elastic deformation occurs in all cases
- No curvature occurs during tensioning and thermal expansion

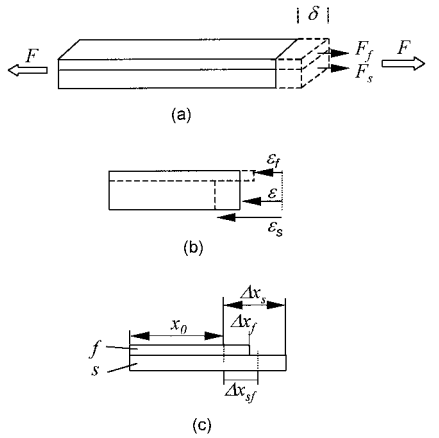


**Figure A.1** (a) Schematic of a two-layer (substrate and front coat) composite under tension, (b) cross-sectional view of (a), and (c) schematic of the two-layer composite after thermal expansion.

### Lateral contraction and Poisson's ratio of individual layers

From the experiments, we can obtain data for the substrate and combined layers, for example, S and SF. The goal is to calculate the properties of the front coat (the situation is the same for the back coat). Now consider the two-layer composite plate shown in Figure A.1(a), which has unit width and length, and a thickness of $(f + s)$. When the applied force is $F$, the elongation is $\delta$. We have

$$F = F_f + F_s = \sigma_f A_f + \sigma_s A_x = \sigma_f f + \sigma_s s = E_f \delta f + E_s \delta s \tag{A.1}$$

and

$$F = E_{sf} \delta (f + s) \tag{A.2}$$

where $F_f$, $F_s$, and $F_{sf}$ are the axial forces applied to the front coat, substrate, and the composite layer (substrate plus front coat), respectively. At the same time, the composite plate shows a lateral contraction of $\epsilon = \nu_{sf}\delta$, where $\nu_{sf}$ is the Poisson's ratio of the composite.

If the individual layers were allowed to contract freely (i.e., no bonding exists between the layers), their lateral contractions would be [see Fig. A.1(b)].

$$\varepsilon_f = \nu_f \delta \quad \text{and} \quad \varepsilon_s = \nu_s \delta \tag{A.3}$$

where $\nu_f$ and $\nu_s$ are the Poisson's ratio of the front coat and substrate, respectively.

To keep physical continuity of the interface, a shear force $F^T$ exists at the interface to make both layers' real contractions equal to $\epsilon$.

$$\left.\begin{aligned} F_f^T &= \sigma_f^T f = E_f^T(\varepsilon - \varepsilon_f)f \\ F_s^T &= \sigma_s^T s = E_s^T(\varepsilon - \varepsilon_s)s \\ F_f^T &= -F_s^T \end{aligned}\right\} \quad E_f^T\varepsilon f - E_f^T\varepsilon_f f = E_s^T\varepsilon_s s - E_s^T\varepsilon s \tag{A.4}$$

where the superscript $T$ indicates the property in TD direction. Thus,

$$(E_f^T f + E_s^T s)\varepsilon = E_f^T f\varepsilon_f + E_s^T s\varepsilon_s \tag{A.5}$$

This is different from the rule of mixtures in eq. (5). Using eq. (A.5) and the Young's moduli of substrate and the combined layers in TD, we can calculate the lateral contraction $\epsilon_f$ and Poisson's ratio, $\nu = \epsilon_f/\delta$, of the front coat.

### CTE and CHE of individual layers

With reference to Figure A.1(c), the original linear dimension of the combined layer structure is one ($x_0 = 1$). After a unit temperature increase ($\Delta T = 1$), the structure expands by $\Delta x_{sf}$. If there were not interfacial bonding, the free thermal expansion of the substrate after the temperature increase would be $\Delta x_s$, whereas that of the front layer would be $\Delta x_f$. So there is an interfacial shear stress that causes a $(\Delta x_{sf} - \Delta x_s)$ deformation in the substrate and a $(\Delta x_{sf} - \Delta x_f)$ deformation in the front layer.

$$\sigma = (\Delta x_{sf} - \Delta x_f)E_f f = -(\Delta x_{xf} - \Delta x_s)E_s s \tag{A.6}$$

Given that $\Delta x_s = \alpha_s x_0 \Delta T$, we have

$$E_f f(\alpha_{sf} - \alpha_f) = E_s s(\alpha_s - \alpha_{sf}) \tag{A.7}$$

where $\alpha_s$, $\alpha_f$, and $\alpha_{sf}$ are the CTE of the substrate, front coat, and the composite, respectively.

Using eq. (5),

$$(E_f f + E_s s)\alpha_{sf} = E_f f\alpha_f + E_s s\alpha_s \tag{A.8}$$

and

$$E_{sf}(f + s)\alpha_{sf} = E_f f\alpha_f + E_s s\alpha_s \tag{A.9}$$

This is similar to the shape of the equation for lateral contraction [eq. (A.5)]. We need Young's modulus data at the corresponding temperatures to calculate the CTE of individual layers.

The same methodology can be used to calculate the CHE of individual layers using the data of substrate and combined layers at various relative humidities.

$$E_{sf}(f + s)\mathrm{CHE}_{sf} = E_f f\mathrm{CHE}_f + E_s s\mathrm{CHE}_s \tag{A.10}$$

### Calculation of lateral contraction of magnetic tape as a three-layer composite

The same methodology can be used to calculate the lateral contraction of the magnetic tape as a three-layer composite, if we have the corresponding data for each layer. The final equation is

$$\varepsilon_t = \frac{E_f^T f\varepsilon_f + E_s^T s\varepsilon_s + E_b^T b\varepsilon_b}{E_f^T f + E_s^T s + E_b^T b} \tag{A.11}$$

The result is to be compared to the measured data of the tape, to validate the model.

### References


1. Bhushan, B. Mechanics and Reliability of Flexible Magnetic Media, 2nd ed.; Springer-Verlag: New York, 2000.
2. http://www.lto-technology.com/newsite/html/format.html
3. Richards, D.; Sharrock M. IEEE Trans Magn 1998, 34, 1878.
4. Bhushan, B. Tribology and Mechanics of Magnetic Storage Devices, 2nd ed.; Springer-Verlag: New York, 1996.
5. Bobji, M.; Bhushan, B. J Mater Res 2001, 16, 844.
6. Higashioji, T.; Bhushan, B. J Appl Polym Sci, to appear.
7. Bhushan, B.; Ma, T.; Higashioji, T. J Appl Polym Sci 2002, 83, 2225.
8. Weick, B.; Bhushan, B. J of Information Storage and Processing System 2000, 2, 207.
9. Weick, B.; Bhushan, B. J Appl Poly Sci 2001, 81, 1142.
10. Ma, T.; Bhushan, B. Rev Sci Instr, to appear.
11. Storer, R. A. Annu Book ASTM Stand 1997, 14.02; 1999, 8.02.
12. Chen, D.; Zachmann, H. Polymer 1991, 32, 1612.
13. Jones, R. Mechanics of Composite Materials, 2nd ed.; Taylor & Francis: Philadelphia, 1999.
14. Silva, M.; Spinace, M.; Paoli, M. J Appl Polym Sci 2001, 80, 20.
15. Haghighat, M.; Borhani, S. J Appl Polym Sci 2000, 78, 1923.
16. Gillmor, J.; Greener, J. ANTEC 1997, 45, 1582.
17. Ezuerra, T.; Balta-Calleja, F.; Zachmann, H. Acta Polym 1993, 44, 18.
18. Kumar, G.; Kumar, V.; Madras, G. J Appl Polym Sci 2002, 84, 681.
19. Murooka, H. (Teijin Ltd.); Osawa, T. (DuPont-Teijin Ltd.), personal communication, March 27, 2001.
20. Koseki, M.; Watanabe, H. Eur. Pat. EP 0982115A1, 2000.
21. Ouchi, I.; Hosoi, M.; Tomie, T. Jpn J Appl Phys 1992, 31, 2505.